RSC Advances

PAPER

View Article Online
View Journal | View Issue

Cite this: *RSC Adv.*, 2022, **12**, 13480

Benzo[de]isoquinoline-1,3-dione condensed asymmetric azaacenes as strong acceptors†

Pengxin Zhou, * Lanlan Deng, Zengtao Han, Xiaolong Zhao, Zhe Zhang and Shuhui Huo *

Received 18th February 2022
Accepted 19th April 2022

DOI: 10.1039/d2ra01074g

rsc.li/rsc-advances

We have designed and synthesized three novel benzo[de]isoquinoline-1,3-dione (BQD) condensed asymmetric azaacenes, **BQD-TZ**, **BQD-AP** and **BQD-PA**, with different end groups of 1,2,5-thiadiazole, acenaphthylene and phenanthrene. The triisopropylsilylethynyl groups were grafted to increase the solubility and crystallinity of the three molecules. These molecules have high electron affinity values of 3.87, 3.69 and 3.74 eV for **BQD-TZ**, **BQD-AP** and **BQD-PA**, respectively as confirmed by cyclic voltammetry measurements. Single-crystal X-ray diffraction revealed that these molecules have strong π–π stacking with distances of 3.31–3.41 Å and different stacking arrangements.

Introduction

Conjugated molecules are important organic materials because of their outstanding electronic properties and potential applications in organic electronic devices, such as organic field-effect transistors (OFETs) and organic photovoltaics (OPVs).[1–7] Currently, a large number of p-type semiconductors have been reported with excellent device performance but the n-type semiconductors are still lagging in comparison.[8–14] Therefore, the development of new conjugated molecules with high electron-affinities (EAs) is an important topic in the field of functional π-materials.

N-Heteroacenes are among the most important electron-accepting materials.[15,16] Compared to the acenes, the *N*-heteroacenes include unsaturated N atoms in the conjugated backbone; this can lower both the EA and ionic potential (IP), which is beneficial for stabilizing and achieving electron transport for the resulting molecules.[17–23] For instance, 6,13-bis(triisopropylsilylethynyl)pentacene (TIPS-PEN) is a typical n-type semiconductor. Miao *et al.* introduced four unsaturated N atoms to develop an n-type material of 6,13-bis((triisopropylsilyl)ethynyl)-5,7,12,14-tetraazapentacene (TIPS-TAP), which exhibited electron mobility exceeding 10 $cm^2 V^{-1} s^{-1}$.[24] *N*-heteroacenes usually have large conjugated backbones, which are not beneficial to the structural characteristics and device fabrication *via* solution processing.[25–29] To overcome this issue, triisopropylsilyl (TIPS)-ethynyl groups were introduced by the Stille coupling reaction and the nucleophilic addition reaction.[30–33] The studies showed that TIPS-ethynyl units play a vital role not only in improving the solubility and stability of acenes and heteroacenes but also in enhancing their capability for π-stacked arrays.[34–37] Larger conjugated *N*-heteroacenes have been reported due to the employment of TIPS-ethyl groups.[28,38–41] However, most of the work focuses on the study of symmetric *N*-heteroacenes, and the asymmetric *N*-heteroacenes are rare.

Herein, we report novel benzo[de]isoquinoline-1,3-dione condensed asymmetric azaacenes, which have different end-fused groups. The studies below detail their synthesis, optical and electrochemical properties, and molecular packing, and reveal that the end-fused group plays an important role in tuning the electronic properties and molecular stacking behaviors based on asymmetric azaacenes.

Experimental

Instruments and measurements

^{1}H NMR and ^{13}C NMR spectra of new compounds were recorded on a Varian Mercury-400 Plus or a Varian Mercury-300 Plus and Agilent Technologies DD2 (600 MHz) spectrometer in $CDCl_3$. Chemical shifts (δ) for NMR were quoted in ppm relative to the solvent peak (7.26 ppm for ^{1}H and 77.00 ppm for ^{13}C in $CDCl_3$). High-resolution mass spectra (HRMS) were obtained with a Bruker Daltonics APEXII 47 e FT-ICR, Agilent QTOF 700 or Agilent 1200 spectrometer and Shimadzu MALDI-7090. Thermogravimetric analysis (TGA) was carried out on a Netzsch 5500 thermogravimetry analyser under a nitrogen atmosphere at a flow rate of 100 mL min^{-1-1}, and the heating rate was 10.0 °C min^{-1-1} from ambient temperature to 800 °C. The UV-vis absorption spectra were recorded on a UV-Vis-NIR spectrophotometer (UV-3600 Plus, Shimadzu, Japan). Fluorescence emission spectra were obtained on a steady-state fluorescence spectrometer (Edinburgh Instruments). Cyclic voltammetry

College of Chemistry and Chemical Engineering, Northwest Normal University, Lanzhou 730070, China. E-mail: zhoupx@nwnu.edu.cn; huosh@nwnu.edu.cn

† Electronic supplementary information (ESI) available. CCDC 2150585, 2150586, 2150828. For ESI and crystallographic data in CIF or other electronic format see https://doi.org/10.1039/d2ra01074g

(CV) experiments were performed at room temperature with an electrochemical analyser (CHI 660C, Chenhua Inc., China). Density functional theory (DFT) calculations were performed using the Gaussian 09 program, with the B3LYP hybrid functional and basis set 6-311G (d,p) for the ground-state geometry optimization. Single-crystal data collections were performed with a Bruker Smart Apex CCD X-ray diffractometer (Bruker, Germany) with highly oriented graphite crystal monochromated Mo K_α radiation ($\lambda = 0.071073$ nm) using ω and φ scan modes. Unit cell dimensions were obtained with least-squares refinements, and semi-empirical absorption corrections were applied using the SADABS program. The structures were solved by the direct method and refined by the full-matrix least-squares technique based on F^2 with the SHELXTL-97 program. All of the atoms were obtained from difference Fourier maps, and all nonhydrogen atoms were refined with atomic anisotropic thermal parameters.

Synthetic procedures

All reagents and chemicals were used as received from commercial sources without further purification. Compounds **6**, **7** and **9** were synthesized according to the literature.[30]

***N*^{5},*N*^{5},*N*^{6},*N*^{6}-Tetramethyl-1,2-dihydroacenaphthylene-5,6-dicarboxamide (2).** 1,2-Dihydroacenaphthylene (4.8 g, 31.12 mmol) was dissolved in 50 mL of chlorobenzene. The solution was then cooled to 0 °C, and then dimethyl carbamoyl chloride (8.8 g, 81.84 mmol) and $AlCl_3$ (11.2 g, 84 mmol) were slowly added, successively. The mixture was heated to 110 °C for 12 h. After cooling to room temperature, the mixture was poured into 200 mL of cold aqueous hydrochloric acid solution (5%). The solution was extracted with methylene chloride and subsequently washed with sodium bicarbonate solution and water. The combined organic layers were dried with $MgSO_4$ and filtered. The solvent was removed. Compound **2** (8.54 g, 91%) was obtained by recrystallization from chlorobenzene solution. ^{1}H NMR (400 MHz, $CDCl_3$) δ 7.37 (d, $J = 7.2$ Hz, 1H), 7.30 (d, $J = 7.2$ Hz, 1H), 3.40 (s, 2H), 3.08 (s, 3H), 2.86 (s, 3H). ^{13}C NMR (151 MHz, $CDCl_3$) δ 171.4, 147.6, 139.9, 130.1, 127.7, 125.0, 119.5, 77.4, 77.2, 76.9, 39.4, 35.0, 30.3.

1,2-Dihydroacenaphthylene dicarboxylic acid anhydride (3). In a 100 mL round-bottomed flask, compound **2** (8.5 g, 28.7 mmol) was suspended in 20 mL of concentrated hydrochloric acid. The mixture was heated to reflux for 4–5 h. The solution was then cooled to room temperature. The off-white precipitate was collected by filtration and washed with cold water and purified by column chromatography, eluting with petroleum ether/ethyl acetate (from 4 : 1 to 2 : 1) to obtain the product (5.7 g, 89%). ^{1}H NMR (400 MHz, $CDCl_3$) δ 8.49 (d, $J = 5.5$ Hz, 2H), 7.61 (d, $J = 5.0$ Hz, 2H), 3.61 (s, 4H). ^{13}C NMR (151 MHz, $CDCl_3$) δ 160.8, 155.7, 138.0, 134.9, 129.1, 121.5, 115.4, 31.9.

***N*-Hexyldecyl-1,2-dihydroacenaphthylene dicarboxylic acid imide (3).** Under N_2, compound **2** (3.0 g, 13.38 mmol) was dissolved in 50 mL of ethanol and heated to reflux for 1 h. The solution was cooled back to room temperature, and *N*-hexylamine (1.61 g, 15.91 mmol) was added dropwise. The solution was then heated to 80 °C for 12 h and water was added to quench the reaction. The organic phase was extracted with chloroform, washed with water and brine, and dried over sodium sulfate. After the removal of the solvents, the crude materials were further purified by column chromatography with petroleum ether/ethyl acetate (5 : 1) to give the product. Yield (3.06 g, 75%). ^{1}H NMR (400 MHz, $CDCl_3$) δ 8.49 (d, $J = 7.2$ Hz, 2H), 7.55 (d, $J = 7.6$ Hz, 2H), 4.17 (t, $J = 7.6$ Hz 2H), 3.56 (s, 4H), 1.76–1.67 (m, 2H), 1.47–1.39 (m, 2H), 1.39–1.30 (m, 4H), 0.88 (t, $J = 7.0$ Hz, 3H). ^{13}C NMR (150 MHz, $CDCl_3$) δ 164.4, 153.6, 137.7, 132.6, 126.4, 120.8, 119.3, 77.2, 77.0, 76.8, 40.3, 31.61 (d, $J = 9.6$ Hz), 28.2, 26.86, 22.6, 14.0.

2-Hexyl-1*H*-indeno[6,7,1-def]isoquinoline-1,3,6,7(2*H*)-tetraone (4). Compound **3** (3 g, 9.7 mmol) and CrO_3 (4.79 g, 47.87 mmol) were dissolved in acetic anhydride. The mixture was stirred vigorously at room temperature until CrO_3 was completely dissolved. The system was heated to 110 °C for 30 min. The reaction system was poured into ice and mixed with dilute hydrochloric acid to precipitate solids. The organic phase was extracted with dichloromethane and washed with saturated sodium chloride solution. After the removal of the solvents, the crude materials were further purified by column chromatography with petroleum ether/dichloromethane (1 : 2) as the eluent. Yield (2.54 g, 78%). ^{1}H NMR (400 MHz, $CDCl_3$) δ 8.81 (d, $J = 7.2$ Hz, 2H), 8.35 (d, $J = 7.6$ Hz, 2H), 4.22 (t, $J = 7.6$ Hz 2H), 1.79–1.71 (m, 2H), 1.47–1.41 (m, 2H), 1.38–1.33 (m, 4H), 0.90 (t, $J = 7.0$ Hz, 3H). ^{13}C NMR (150 MHz, $CDCl_3$) δ 186.2, 162.5, 143.7, 132.0, 126.8, 126.1, 122.9, 41.1, 31.5, 28.0, 26.7, 22.5, 14.0. HRMS (ESI): m/z $[M + Na]^+$ calc. for $C_{20}H_{17}NO_4Na$: 358.10420; found: 358.10476.

2-Hexyl-7,11-bis((triisopropylsilyl)ethynyl)-1*H*-pyrido[3′,4′,5′:5,6]acenaphtho[1,2-b][1,2,5] thiadiazolo[3,4-g]quinoxaline-1,3(2*H*)-dione (BQD-TZ). Compound **6** (200 mg, 0.379 mmol) and compound **5** (189.24 mg, 0.564 mmol) were added to the acetic acid (20 mL), the mixture was heated to 90 °C and stirred for 12 h under nitrogen. The reaction system was then cooled to room temperature and poured into 100 mL of 5% aqueous NaOH, the mixture was extracted with dichloromethane (3 × 50 mL). The combined organic phases were dried with $MgSO_4$ and filtered. The filtrate was concentrated and purified by column chromatography, eluting with petroleum ether/dichloromethane (4 : 1) to give **BQD-TZ** (244 mg, 78%). ^{1}H NMR (400 MHz, $CDCl_3$) δ 8.76 (d, $J = 7.2$ Hz, 2H), 8.46 (d, $J = 6.4$ Hz, 2H), 4.21 (t, $J = 7.6$ Hz, 2H), 1.83–1.69 (m, 2H), 1.34 (d, $J = 4.5$ Hz, 42H), 1.25 (s, 6H), 0.91 (t, $J = 6.8$ Hz, 3H). ^{13}C NMR (150 MHz, $CDCl_3$) δ 163.1, 155.4, 154.6, 141.9, 137.6, 136.2, 132.7, 125.4, 124.7, 122.7, 115.9, 110.5, 100.6, 31.5, 29.7, 28.2, 26.8, 22.6, 18.9, 14.0, 11.6. HRMS (ESI): m/z $[M + H]^+$ calc. for $C_{48}H_{60}N_5O_2SSi_2$: 826.39848; found: 826.39844.

2-Hexyl-7,16-bis((triisopropylsilyl)ethynyl)-1*H*-acenaphtho[1′,2′:5,6]pyrazino[2,3-g]pyrido[3′,4′,5′:5,6]acenaphtho[1,2-*b*]quinoxaline-1,3(2*H*)-dione (BQD-AP). Compound **7** (200 mg, 0.297 mmol) was dissolved in 10 mL of dried tetrahydrofuran under nitrogen. $LiAlH_4$ (1 M) (5.94 mL, 5.94 mmol) was added to the system dropwise. The solution was stirred for 2 h at 0 °C, and then for 12 h at room temperature. The reaction mixture was added dropwise into 50 mL of water after stopping.

Subsequently, the solution was extracted with methylene chloride (3 × 20 mL). The combined organic layers were dried with $MgSO_4$ and filtered. The solvent was removed under reduced pressure to give the corresponding crude diamine **8** as a deep red oil, which was purified by column chromatography, eluting with petroleum ether/dichloromethane (from 3 : 1 to 2 : 1) to give the corresponding product **8**. This crude product was also directly added to acetic acid (10 mL) solutions of the corresponding diketones (148 mg, 0.442 mmol). The mixtures were heated to 110 °C for 7 h under argon. After cooling to room temperature, the mixture was poured into 100 mL of 5% aqueous NaOH and extracted with dichloromethane (3 × 50 mL). The combined organic phases were dried with $MgSO_4$ and filtered. The solvent was concentrated and purified by column chromatography, eluting with petroleum ether/dichloromethane (from 2 : 1 to 1 : 1) to give the desired product **BQD-AP** (166 mg, 59%). ^{1}H NMR (300 MHz, $CDCl_3$) δ 8.74 (d, J = 7.5 Hz, 2H), 8.45 (t, J = 6.8 Hz, 4H), 8.15 (d, J = 8.1 Hz, 2H), 7.91 (t, J = 7.5 Hz, 2H), 4.11 (t, J = 7.5 Hz, 2H), 1.77–1.67 (m, 2H), 1.45 (s, 48H), 1.34 (s, 6H), 0.90 (t, J = 6.6 Hz, 3H). ^{13}C NMR (75 MHz, $CDCl_3$) δ 163.2, 155.8, 155.0, 142.6, 141.4, 138.5, 136.8, 136.7, 136.5, 132.7, 131.5, 130.1, 129.0, 125.3, 124.5, 123.9, 122.8, 122.6, 109.0, 101.2, 40.7, 31.5, 28.2, 26.8, 22.6, 19.0, 14.0, 11.8. HRMS (MALDI-TOF) m/z: $[M + H]^+$ calcd for $C_{60}H_{66}N_5O_2Si_2$, 945.380; found, 945.310.

2-Hexyl-7,18-bis((triisopropylsilyl)ethynyl)-1*H*-dibenzo[*a*,*c*]pyrido[3″,4″,5″″:5′,6′]acenaphtho [1′,2′:5,6]pyrazino[2,3-*i*]phenazine-1,3(2*H*)-dione (BQD-PA). Compound **9** (200 mg, 0.286 mmol) was dissolved in 10 mL of dried tetrahydrofuran under nitrogen. $LiAlH_4$ (1 M) (5.74 mL, 5.74 mmol) was added to the system dropwise. The solution was stirred for 2 h at 0 °C, and then for 12 h at room temperature. The reaction mixture was added dropwise into 50 mL of water after stopping. Subsequently, the solution was extracted with methylene chloride (3 × 20 mL). The combined organic layers were dried with $MgSO_4$ and filtered. The solvent was removed under reduced pressure to give the corresponding crude diamine 10 as a deep red oil, which was purified by column chromatography, eluting with petroleum ether/dichloromethane (from 3 : 1 to 2 : 1) to give the corresponding product of **10**. This crude product was also directly added to an acetic acid (10 mL) solution of the corresponding diketone (142 mg, 0.426 mmol). The mixture was heated to 110 °C for 7 h under argon. After cooling to room temperature, the mixture was poured into 100 mL of 5% aqueous NaOH and extracted with dichloromethane (3 × 50 mL). The combined organic phases were dried with $MgSO_4$ and filtered. The solvent was concentrated and purified by column chromatography, eluting with petroleum ether/dichloromethane (from 2 : 1 to 1 : 1) to give the final product **BQD-PA** (190 mg, 68%).^{1}H NMR (300 MHz, $CDCl_3$) δ 9.63 (d, J =

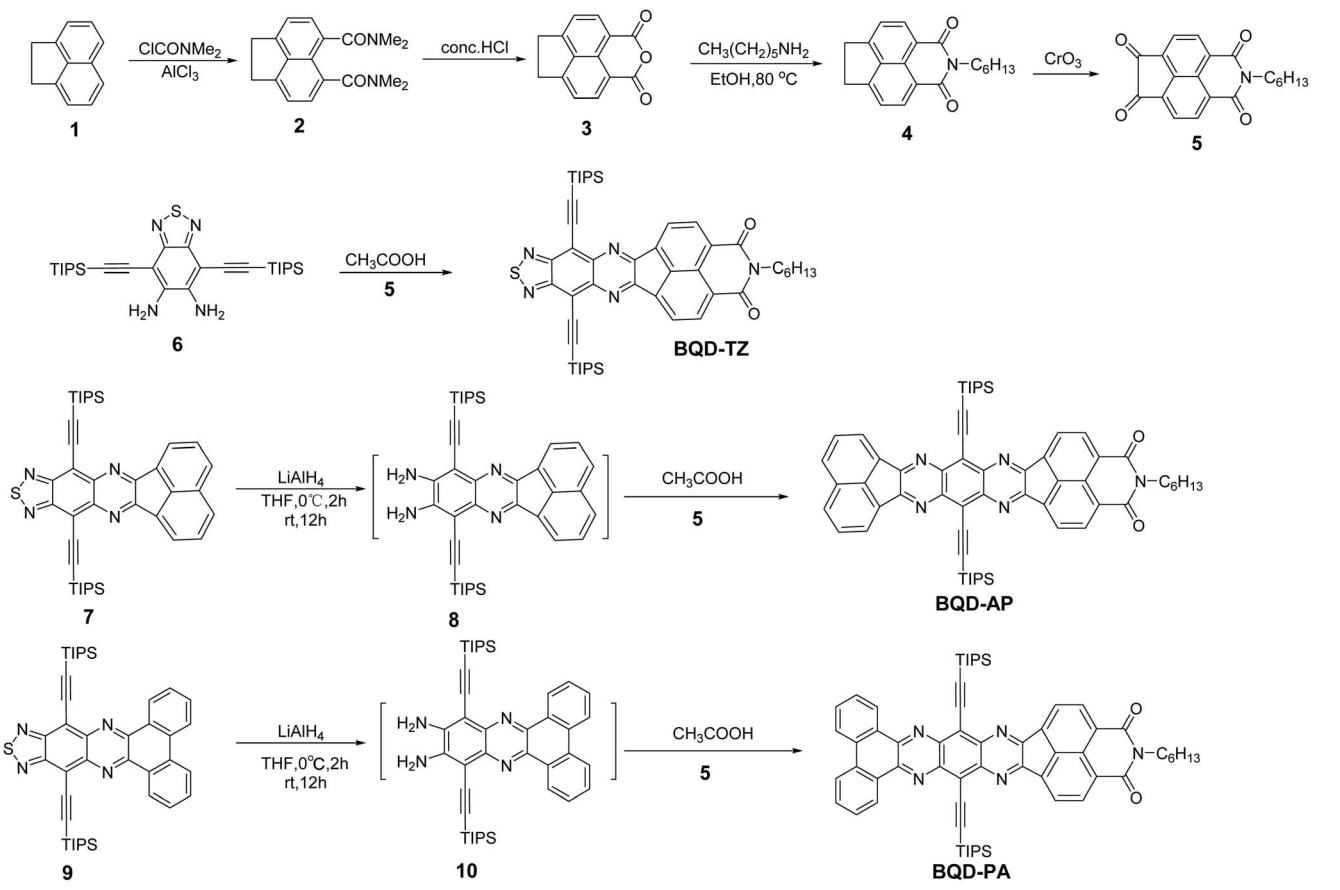

Scheme 1 Synthetic routes for BQD-TZ, BQD-AP and BQD-PA.

7.2 Hz, 2H), 8.75 (d, $J = 7.2$ Hz, 2H), 8.54 (d, $J = 7.8$ Hz, 2H), 8.47 (d, $J = 7.2$ Hz, 2H), 7.86 (t, $J = 7.9$ Hz, 2H), 7.75 (t, $J = 6.6$ Hz, 2H), 4.16 (t, $J = 7.4$ Hz 2H), 1.79–1.70 (m, 2H), 1.48 (s, 42H), 1.37 (s, 6H), 0.92 (t, $J = 6.3$ Hz, 3H). ^{13}C NMR (75 MHz, $CDCl_3$) δ 163.1, 155.2, 144.4, 142.2, 142.0, 137.0, 136.7, 132.8, 132.7, 131.5, 130.1, 128.1, 127.5, 125.3, 124.5, 123.4, 123.0, 122.7, 109.7, 101.6, 40.8, 31.5, 28.2, 26.8, 22.6, 19.0, 14.0, 11.9. HRMS (MALDI-TOF) m/z: $[M + H]^+$ calc. for $C_{62}H_{68}N_5O_2Si_2$, 971.420; found, 971.315.

Synthesis and electronic properties

The synthetic routes of three asymmetric azaacenes are illustrated in Scheme 1. Compound **2** was synthesized from the commercial starting material 1,2-dihydroacenaphthylene by Friedel–Crafts acylation. Compound **2** was then subjected to acidolysis and dehydration to form anhydride **3**, which was then transformed into compound **4** by a condensation reaction. Compound **4** was oxidized to give the key intermediate of diketone **5**. The condensation reaction was conducted between compound **4** and compound **5** to give the desired asymmetric azaacene of **BQD-TZ**. Compounds **7** and **9** were reduced to the corresponding diamine compounds by $LiAlH_4$ in a dry THF solution. Finally, the **BQD-AP** and **BQD-PA** were also synthesized by a similar reaction to that of **BQD-TZ**. These compounds have good solubility in common organic solvents such as dichloromethane and chloroform and exhibit excellent thermal stability, with 5% weight loss upon heating up to 368 °C for **BQD-TZ**, 407 °C for **BQD-AP**, and 395 °C for **BQD-PA** (Fig. S1†).

The absorption and emission spectra of three molecules were recorded in dilute dichloromethane solution ($c = 10^{-5}$ M, Fig. 1a). **BQD-TZ** exhibited a similar absorption profile to the previously reported compounds **7** and **9**.[30] When the end groups were changed from 1,2,5-thiadiazole to acenaphthylene and phenanthrene, the absorption region at 350 nm to 400 nm showed significant differences where the absorption wavelength was gradually red-shifted as π-conjugation increased. This was because this region is contributed by π–π* transitions of the conjugated aromatic segments.[42] The maximum absorption wavelengths (λ_{max}) of these molecules are 548, 519, and 554 nm for **BQD-TZ**, **BQD-AP** and **BQD-PA**, respectively. This is attributed to the fused aromatic structures, considering that the three molecules differ only in the electron-donating nature of the aromatic-ring unit. Compared to **BQD-TZ** and **BQD-PA**, although the λ_{max} of the **BQD-AP** has a blue-shift, its emission spectrum shows the largest wavelength, indicating that **BQD-AP** has the largest Stokes shift as shown in Fig. 1b and Table 1.

The electron affinities (EA) of these molecules were studied by cyclic voltammetry (CV).[43] The three compounds exhibited reversible reduction peaks in solution (Fig. 2). Electron affinity (EA) values were estimated from the onsets of the first reduction peak, while the potentials were determined using ferrocene (Fc) as the standard, by empirical formulas, $EA = (E_{red}^{onset} - E_{Fc/Fc}^{+1/2} + 4.8)$ eV. The 1,2,5-thiadiazole containing **BQD-TZ** had the highest EA value of 3.87 eV, while **BQD-PA**, with phenanthrene, had a slightly higher EA value of 3.74 eV. The major reason is that 1,2,5-thiadiazole is a stronger electron-accepting group as compared to acenaphthylene. When the acenaphthylene was changed to phenanthrene, the conjugated skeleton was enlarged, the electron density was better distributed on the entire conjugated skeleton, and therefore, the **BQD-AP** provided the lowest EA value of 3.69 eV. It should be noted that the EA values of these molecules are higher than those of most *N*-

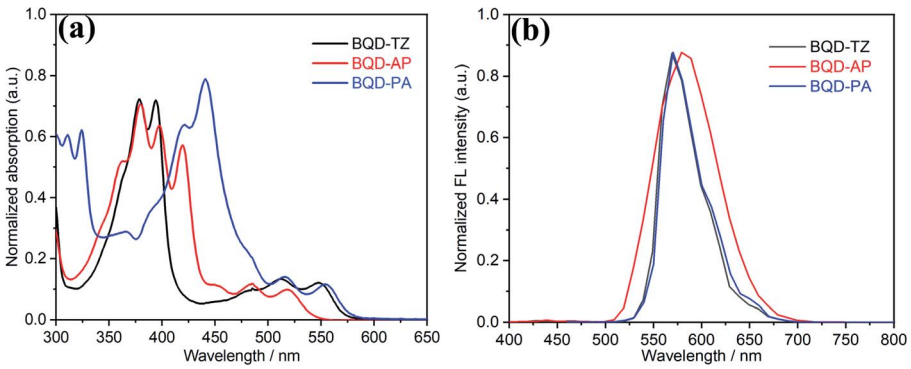

Fig. 1 UV-Vis absorption (a) and fluorescence (b) spectra of **BQD-TZ**, **BQD-AP** and **BQD-PA** in dichloromethane.

Table 1 Photophysical and electrochemical properties of **BQD-TZ**, **BQD-AP** and **BQD-PA**

Compound	Band I[a] (nm)	Band II[a] (nm)	λ_{abs}/nm (log ε) [a]	λ_{em}[a,b]/nm	Stokes shift/nm	E_{opt}[a]/eV	EA[c]/eV	LUMO[d]/eV	E_g[d]/eV
BQD-TZ	350–400	500–570	548 (7.8×10^4)	569	21	2.12	3.87	−3.43	2.35
BQD-AP	350–475	480–530	519 (6.4×10^4)	579	60	2.21	3.69	−3.06	2.55
BQD-PA	425–475	500–570	554 (8.1×10^4)	569	15	2.10	3.74	−3.19	2.44

[a] Dissolved in dichloromethane ($c = 10^{-5}$ M). [b] Excitation wavelengths for the emission measurements are 548, 519, and 554 nm for **BQD-TZ**, **BQD-AP** and **BQD-PA**. [c] EA was measured by CV. [d] Calculated energy levels using B3LYP/6-31G, (d, p) ΔE_g = LUMO–HOMO.

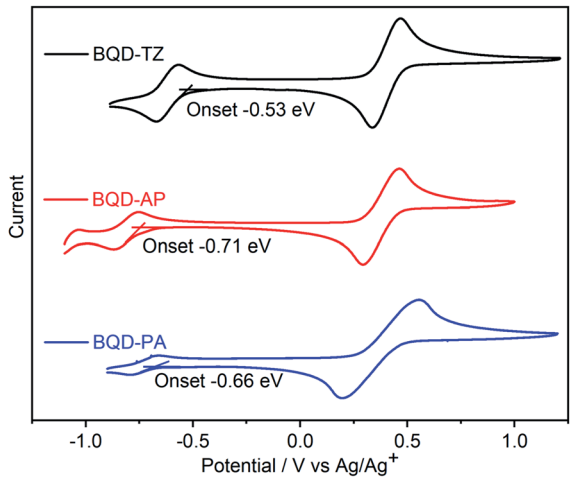

Fig. 2 The reduction curves of BQD-TZ, BQD-AP and BQD-PA in dichloromethane.

heteroarenes due to the introduction of the strong electron-accepting unit of benzo[de]isoquinoline-1,3-dione.[32,44–46] These results suggest that by attaching different electron-donating groups, the electron-deficient nature of the azaacene can easily be tuned. In order to combine these results with theoretical predictions, density functional theory (DFT, B3LYP, 6-31G (d,p)) calculations were carried out. The DFT results demonstrated that theoretical predictions exhibited the same tendency as the experimental data by analyzing LUMO levels (−3.43 eV for **BQD-TZ**, −3.00 eV for **BQD-AP**, −3.19 eV for **BQD-PA**, Fig. S2†). It is beneficial for us to predict the electronic properties of such new azaacene derivatives in line with the experimental findings. As shown in Fig. S2,† for the HOMO levels, the three compounds have similar electron density distributions along the conjugated backbone, while for the LUMO levels, the electron density of **BQD-AP** is mainly distributed on the BQD part, and the electron densities of **BQD-TZ** and **BQD-PA** are poor on the BQD part. This might be the main reason why even though **BQD-PA** has a similar chemical structure to **BQD-AP**, its absorption and emission spectra are much more similar to those of **BQD-TZ** than those of **BQD-AP**.

Crystal structure analysis

Single-crystal analysis of molecules is a vital requirement to understand their electronic properties. Single-crystals of three molecules were obtained by slow evaporation from chloroform at room temperature. All of them were examined from X-ray analysis. Their single-crystals are presented in Fig. 3, and the corresponding data are collected in Table S1 (see ESI†). **BQD-TZ** and **BQD-PA** crystallize in the triclinic crystal system with space group $P\bar{1}$ containing two molecules per unit cell. **BQD-AP** crystallizes in the monoclinic crystal system with space group $I2/m$ containing four **BQD-AP** units per unit cell. The three molecules have a nearly planar conjugated backbone and an axisymmetric structure. It can be seen from the unit cell stacking that there is a strong π–π interaction between the molecules of these three substances. **BQD-TZ** has the shortest π-stacking distances of 3.31 Å, suggesting it has the strongest π–π interaction. Introducing the phenanthrene unit slightly increases the π–π

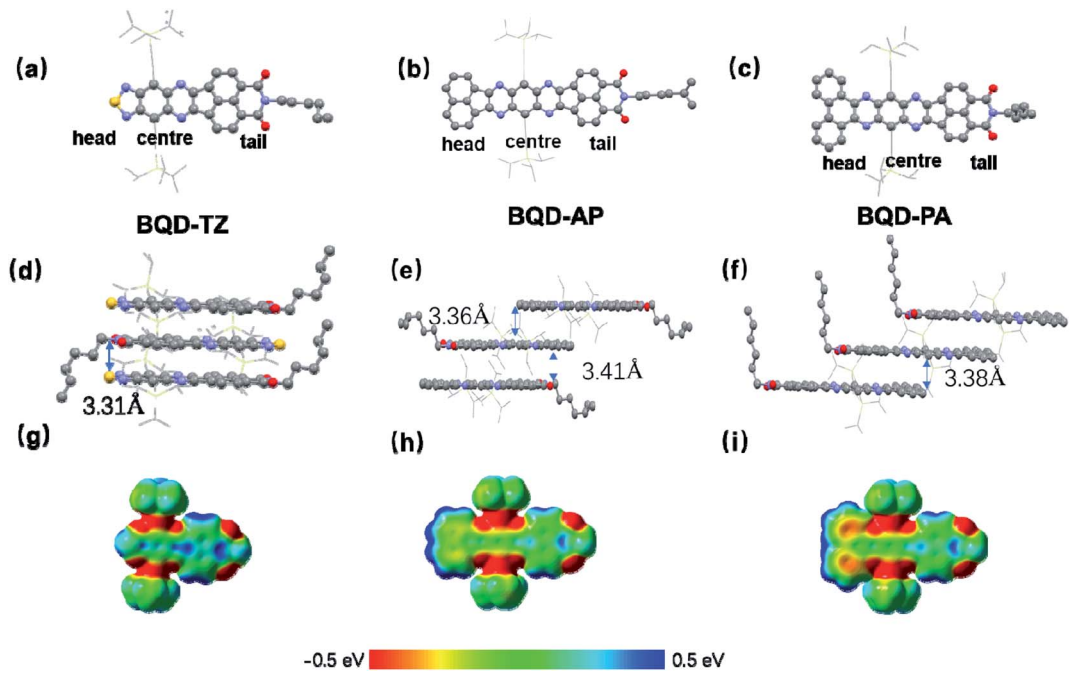

Fig. 3 Molecular single-crystal structure of BQD-TZ (a), BQD-AP (b) and BQD-PA (c). The packing of BQD-TZ (d), BQD-AP (e) and BQD-PA (f); view along the *b*-axis. The packing of BQD-TZ (g), BQD-AP (h) and BQD-PA (f); viewed along the *a*-axis. The conjugated cores are shown with ball-stick models and the silylethynyl substituents are shown with wireframe models. Hydrogen atoms were removed for clarity. Carbon, nitrogen, oxygen, sulfur and silicon atoms are shown in grey, purple, red, orange, and yellow, respectively.

distances to 3.38 Å. The largest distances of 3.36 and 3.41 Å for **BQD-AP** indicate that it possesses the weakest π–π interactions among these molecules. Therefore, the three molecules form a stable, ordered spatial packing. Additionally, the three molecules exhibit very interesting molecular stacking behaviour due to the different end groups. BQD-TA shows the head-to-tail π–π stacking, **BQD-PA** displays tail-to-centre π–π stacking, and **BQD-AP** presents the mixture of head-to-tail and tail-to-centre π–π stacking. To understand this issue, the molecular electrostatic potentials (ESPs) of the three molecules were calculated by DFT with the basis set of B3LYP, 6-31G (d,p). For **BQD-TZ**, the naphthalene unit and the center unit show strong positive and negative ESP, respectively, which make them form strong intermolecular interactions. This is in agreement with its molecular stacking in the single-crystal structure where the naphthalene unit forms strong π–π interactions with the center part. When the end group was changed from 1,2,5-thiadiazole to phenanthrene, **BQD-PA** showed stronger positive ESP in phenanthrene than that of naphthalene; therefore, the center unit is prone to forming π–π with phenanthrene as compared to naphthalene. This is why we only find the tail-to-center π–π stacking in **BQD-PA**. However, when the end group was changed from 1,2,5-thiadiazole to acenaphthylene, the **BQD-AP** also showed the strongest positive and negative ESP in acenaphthylene and center units. The acenaphthylene has a similar molecular size but opposite ESP as compared to the BQD unit, which causes acenaphthylene to form intermolecular interactions with both the center and BQD units. Considering that the center unit has a stronger negative ESP than that of the BQD unit, acenaphthylene forms a stronger intermolecular interaction with the center unit than the BQD unit. This might be the reason the π–π tail-to-center distance (3.36 Å) is slightly smaller than that of π–π head-to-tail distance (3.41 Å) in **BQD-AP**. Overall, the tuning of the end group in asymmetric *N*-heteroacenes is a useful strategy for controlling molecular self-organization behaviours.

Conclusions

In conclusion, we have successfully synthesized three novel benzo[de]isoquinoline-1,3-dione (BQD) condensed asymmetric azaacenes, **BQD-TZ**, **BQD-AP** and **BQD-PA**, which have good solubility and high stability. The X-ray single-crystal structure shows that the three molecules have a nearly planar conjugated backbone and strong π–π stacking with distances from 3.31–3.41 Å, which facilitate desirable solid-state molecular packing. Changing the fused aromatic unit in the benzo[de]isoquinoline-1,3-dione condensed asymmetric azaacenes affected the molecule's optoelectronic properties. Cyclic voltammetry results showed that these molecules possess high electron affinity values that are positive for **BQD-TZ**, **BQD-AP** and **BQD-PA**, respectively.

Conflicts of interest

There are no conflicts to declare.

Acknowledgements

This research was financially supported by the National Natural Science Foundation of China (No. 21462036, 22066021), West Light Foundation of the Chinese Academy of Sciences (2021) and Industrial Support Plan Project of Colleges in Gansu Province (2021CYZC-17).

References

1 R. Dheepika, S. Sonalin, P. M. Imran and S. Nagarajan, *J. Mater. Chem. C*, 2018, **6**, 6916–6919.
2 H. N. Tsao, D. M. Cho, I. Park, M. R. Hansen, A. Mavrinskiy, D. Y. Yoon, R. Graf, W. Pisula, H. W. Spiess and K. Mullen, *J. Am. Chem. Soc.*, 2011, **133**, 2605–2612.
3 S. Zhang, Y. Guo, Y. Zhang, R. Liu, Q. Li, X. Zhan, Y. Liu and W. Hu, *Chem. Commun.*, 2010, **46**, 2841–2843.
4 S. Yang, D. Liu, X. Xu and Q. Miao, *Chem. Commun.*, 2015, **51**, 4275–4278.
5 A. Naibi Lakshminarayana, A. Ong and C. Chi, *J. Mater. Chem. C*, 2018, **6**, 3551–3563.
6 J. Niklas and O. G. Poluektov, *Adv. Energy Mater.*, 2017, **7**, 1602226.
7 B. L. Hu, K. Zhang, C. An, W. Pisula and M. Baumgarten, *Org. Lett.*, 2017, **19**, 6300–6303.
8 M. Müller, L. Ahrens, V. Brosius, J. Freudenberg and U. H. F. Bunz, *J. Mater. Chem. C*, 2019, **7**, 14011–14034.
9 E. C. Rudiger, S. Koser, F. Rominger, J. Freudenberg and U. H. F. Bunz, *Chemistry*, 2018, **24**, 9919–9927.
10 Q. Ye and C. Chi, *Chem. Mater.*, 2014, **26**, 4046–4056.
11 S. N. Sanders, E. Kumarasamy, A. B. Pun, K. Appavoo, M. L. Steigerwald, L. M. Campos and M. Y. Sfeir, *J. Am. Chem. Soc.*, 2016, **138**, 7289–7297.
12 E. C. Rudiger, M. Muller, S. Koser, F. Rominger, J. Freudenberg and U. H. F. Bunz, *Chemistry*, 2018, **24**, 1036–1040.
13 J. E. Anthony, A. Facchetti, M. Heeney, S. R. Marder and X. Zhan, *Adv. Mater.*, 2010, **22**, 3876–3892.
14 H. Usta, A. Facchetti and T. J. Marks, *Acc. Chem. Res.*, 2011, **44**, 501–510.
15 V. Lami, D. Leibold, P. Fassl, Y. J. Hofstetter, D. Becker-Koch, P. Biegger, F. Paulus, P. E. Hopkinson, M. Adams, U. H. F. Bunz, S. Huettner, I. Howard, A. A. Bakulin and Y. Vaynzof, *Sol. RRL*, 2017, **1**, 1700053.
16 S. Zhou, C. An, T. Stelzig, S. R. Puniredd, X. Guo, W. Pisula and M. Baumgarten, *New J. Chem.*, 2015, **39**, 6765–6770.
17 P. Biegger, O. Tverskoy, F. Rominger and U. H. Bunz, *Chemistry*, 2016, **22**, 16315–16322.
18 P. Biegger, M. Schaffroth, O. Tverskoy, F. Rominger and U. H. Bunz, *Chemistry*, 2016, **22**, 15896–15901.
19 M. Muller, H. Reiss, O. Tverskoy, F. Rominger, J. Freudenberg and U. H. F. Bunz, *Chemistry*, 2018, **24**, 12801–12805.
20 S. Yang, B. Shan, X. Xu and Q. Miao, *Chemistry*, 2016, **22**, 6637–6642.
21 M. Ganschow, S. Koser, S. Hahn, F. Rominger, J. Freudenberg and U. H. Bunz, *Chemistry*, 2017, **23**, 4415–4421.

22 J. I. Martinez, J. P. Mora-Fuentes, M. Carini, A. Saeki, M. Melle-Franco and A. Mateo-Alonso, *Org. Lett.*, 2020, **22**, 4737–4741.
23 H. Reiss, L. Ji, J. Han, S. Koser, O. Tverskoy, J. Freudenberg, F. Hinkel, M. Moos, A. Friedrich, I. Krummenacher, C. Lambert, H. Braunschweig, A. Dreuw, T. B. Marder and U. H. F. Bunz, *Angew. Chem., Int. Ed.*, 2018, **57**, 9543–9547.
24 X. Xu, Y. Yao, B. Shan, X. Gu, D. Liu, J. Liu, J. Xu, N. Zhao, W. Hu and Q. Miao, *Adv. Mater.*, 2016, **28**, 5276–5283.
25 D. Cortizo-Lacalle, C. Gozalvez, M. Melle-Franco and A. Mateo-Alonso, *Nanoscale*, 2018, **10**, 11297–11301.
26 P.-Y. Gu, Z. Wang, G. Liu, H. Yao, Z. Wang, Y. Li, J. Zhu, S. Li and Q. Zhang, *Chem. Mater.*, 2017, **29**, 4172–4175.
27 B. Kohl, F. Rominger and M. Mastalerz, *Angew. Chem., Int. Ed.*, 2015, **54**, 6051–6056.
28 B.-L. Hu, K. Zhang, C. An, D. Schollmeyer, W. Pisula and M. Baumgarten, *Angew. Chem., Int. Ed.*, 2018, **57**, 12375–12379.
29 Z. Wang, P. Gu, G. Liu, H. Yao, Y. Wu, Y. Li, G. Rakesh, J. Zhu, H. Fu and Q. Zhang, *Chem. Commun.*, 2017, **53**, 7772–7775.
30 C. An, S. Zhou and M. Baumgarten, *Cryst. Growth Des.*, 2015, **15**, 1934–1938.
31 C. An, X. Guo and M. Baumgarten, *Cryst. Growth Des.*, 2015, **15**, 5240–5245.
32 P. Biegger, M. Schaffroth, K. Brödner, O. Tverskoy, F. Rominger and U. H. F. Bunz, *Chem. Commun.*, 2015, **51**, 14844–14847.
33 S. Miao, A. L. Appleton, N. Berger, S. Barlow, S. R. Marder, K. I. Hardcastle and U. H. F. Bunz, *Chem. - Eur J.*, 2009, **15**, 4990–4993.
34 J. E. Anthony, J. S. Brooks, D. L. Eaton and S. R. Parkin, *J. Am. Chem. Soc.*, 2001, **123**, 9482–9483.
35 B. D. Lindner, J. U. Engelhart, O. Tverskoy, A. L. Appleton, F. Rominger, A. Peters, H.-J. Himmel and U. H. F. Bunz, *Angew. Chem., Int. Ed.*, 2011, **50**, 8588–8591.
36 M. L. Tang, A. D. Reichardt, N. Miyaki, R. M. Stoltenberg and Z. Bao, *J. Am. Chem. Soc.*, 2008, **130**, 6064–6065.
37 M. L. Tang, A. D. Reichardt, P. Wei and Z. Bao, *J. Am. Chem. Soc.*, 2009, **131**, 5264–5273.
38 B.-L. Hu, C. An, M. Wagner, G. Ivanova, A. Ivanova and M. Baumgarten, *J. Am. Chem. Soc.*, 2019, **141**, 5130–5134.
39 C. Wang, J. Zhang, G. Long, N. Aratani, H. Yamada, Y. Zhao and Q. Zhang, *Angew. Chem., Int. Ed.*, 2015, **54**, 6292–6296.
40 Q. Zhang, W. Chen, X. Li, G. Long, W. Gao, Y. Li, R. Ganguly, M. Zhang, N. Aratani, H. Yamada and M. Liu, *Angew. Chem.*, 2018, **130**, 13743–13747.
41 R. K. Dubey, M. Melle-Franco and A. Mateo-Alonso, *J. Am. Chem. Soc.*, 2021, **143**, 6593–6600.
42 G. Qian, Z. Zhong, M. Luo, D. Yu, Z. Zhang, D. Ma and Z. Y. Wang, *J. Phys. Chem. C*, 2009, **113**, 1589–1595.
43 J.-L. Bredas, *Mater. Horiz.*, 2014, **1**, 17–19.
44 S. Miao, A. L. Appleton, N. Berger, S. Barlow, S. R. Marder, K. I. Hardcastle and U. H. F. Bunz, *Chem. - Eur J.*, 2009, **15**, 4990–4993.
45 Z. X. Liang, Q. Tang, R. X. Mao, D. Q. Liu, J. B. Xu and Q. Miao, *Adv. Mater.*, 2011, **23**, 5514–5518.
46 Z. L. Wang, J. W. Miao, G. K. Long, P. Y. Gu, J. B. Li, N. Aratani, H. Yamada, B. Liu and Q. C. Zhang, *Chem.–Asian J.*, 2016, **11**, 482–485.